

Appendices

APPENDIX A - IMAGE ANALYSIS AND FUNCTIONAL STEREOLOGY

Equations developed by Dr. Alexander Prousevitich

The discrete distribution G_i is defined by continuous number density distribution function $n(V)$. It can be defined with the following relation in a general form for 2D and 3D cases [Prousevitich *et al.*, 2007b]:

$$n(V) = \sum_j N_j^{total} \hat{f}_j(V) \quad (A-1)$$

where N_j^{total} and $\hat{f}_j(V)$ are cumulative number density and distribution density function for mode j .

Considering that the relation between 2D and 3D grain size distribution can be expressed by:

$$g(x)dx = \hat{H} \iint_x^{+\infty} \gamma \frac{x}{z} z f(z) d \frac{x}{z} dz \quad (A-2)$$

From equation (A-1), the stereological conversion of an arbitrary distribution function for a 2D cross-section $g(x)$ can be performed by solving of the first type of the Fredholm form integral equation, in regard of function $f(x)$:

$$g(x) = \hat{H} \int_x^{+\infty} \frac{x}{y} \gamma \frac{x}{z} f(z) dz \quad (A-3)$$

where $g(x)$ and $f(x)$ are G_i in 2D and 3D respectively, x is a linear dimension for grain size, $\gamma(\bar{x})$ is a dimensionless function for a distribution density of cross-section of relative size \bar{x} , defined [Sahagian and Prousevitich, 1998] as $\bar{x} = \frac{x}{x_{max}}$, and

\hat{H} is mean projected height coefficient, defined as ratio of particle mean projected area to its size $\hat{H} = \frac{\bar{H}}{D}$.

APPENDIX B - EFFECTS OF WELDING AND DIAGENESIS

Method

This section proposes a method to calculate the former volume of a vesicular pumice clast population that underwent syn- and/or post-deposition compaction by welding and/or diagenesis.

An important volcanological application of functional stereology is the study of deposits that were compacted by welding or diagenesis. Welding commonly occurs in pumiceous pyroclastic flow deposits (ignimbrites) and some pyroclastic fall deposits, and produces clastic rocks that are inappropriate for sieving [e.g. *Freundt, 1999; Kobberger and Schmincke, 1999; Wilson and Hildreth, 2003; Quane and Russell, 2005; Jutzeler et al., 2010*]. Diagenesis can affect all clastic aggregates and is responsible for converting them to rocks. Pumice clasts may compact during welding and/or diagenesis, partially or fully losing their initial porosity (Fig. B.1a), and becoming fiamme [*Bull and McPhie, 2007*]. Welding and/or diagenetic compaction are here approximated (Fig. B.1c) by flattening by pure volume strain [*Quane and Russell, 2005*]. Diameter modification is mostly effective on the axis parallel to the main stress, because the matrix and other clasts surrounding the fiamme also resist the compaction. More complex deformation that can happen during welding and compaction, including simple shear and torsion of clasts, are not considered here. The size of the original pumice clast cannot be precisely reconstructed from its compacted equivalent because, in most cases, the original degree of vesicularity is unknown. The intensity and style of compaction may also vary depending on the former clast size [*Bull and McPhie, 2007*], and fiamme may not be fully compacted.

The range of expected volume changes accompanies compaction in the middle and upper section of the Crest B-3 bed in the Ohanapecosh Formation. The average fiamme diameter in two dimensions is compared with a reconstructed tri-dimensional diameter for various former vesicularities, assuming a regional diagenetic compaction by volume strain (Fig. B.1). Functional stereology on the fiamme shifts the two-dimensional average diameter towards coarser values, and the same result arises for dense clasts of the same sample. The addition of 40, 60 and 80 vol.% of porosity to the fiamme also increases the average diameter values towards coarser values (Fig. B.1b). In the studied example, the application of the functional stereology method and fiamme “de-flattening” more than doubles the modal diameter of the two-dimensional fiamme, assuming 80 vol.% vesicularity was lost by pure volume strain.

Conclusion

Reconstruction of the volume of the former vesicular pumice allows textural characterisation of compacted deposits. Two-dimensional fiamme size estimates on a cross-section of a compacted volcaniclastic rock can deviate by more than a factor 2 from the modal volume of the original pumice clast aggregate.

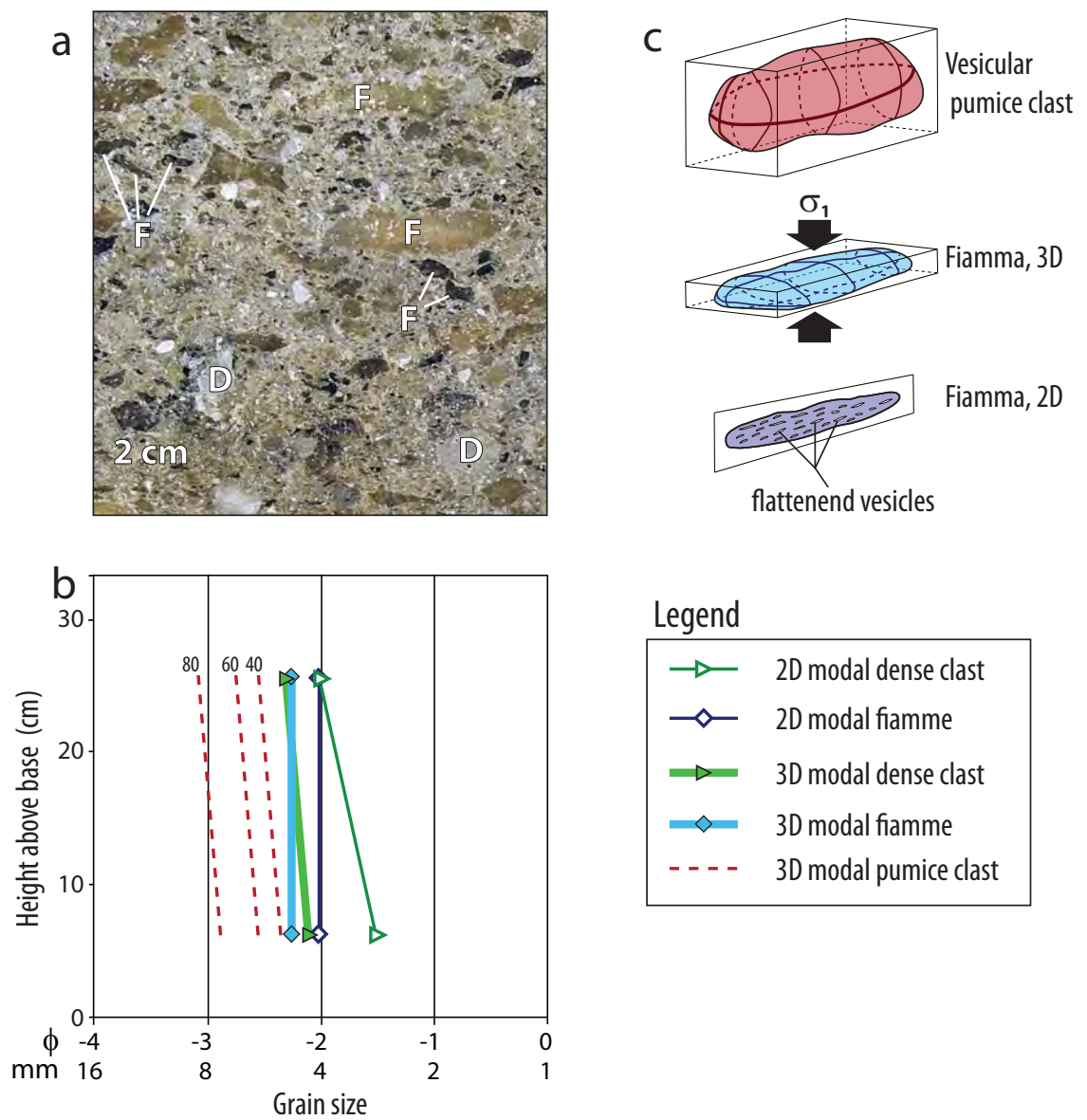


Fig. B.1 Example of the effect of compaction on pumice clasts in middle and upper sections of normally graded andesite breccia to fiamme breccia (facies 12) at Cougar Lake, in the Ohanapecosh Formation. a) Fiamme (F) and dense clast (D) in upper section. Note that dense clasts do not show any alignment compared to fiamme; b) Modal grain sizes of fiamme, dense clasts and "reconstituted" pumice clasts. Numbers 40, 60 and 80 refer to assumed lost vesicularity in vol.%; c) Representation of pumice clast compaction to fiamme by pure strain, with principal stress σ_1

APPENDIX C - OHANAPECOSH FORMATION

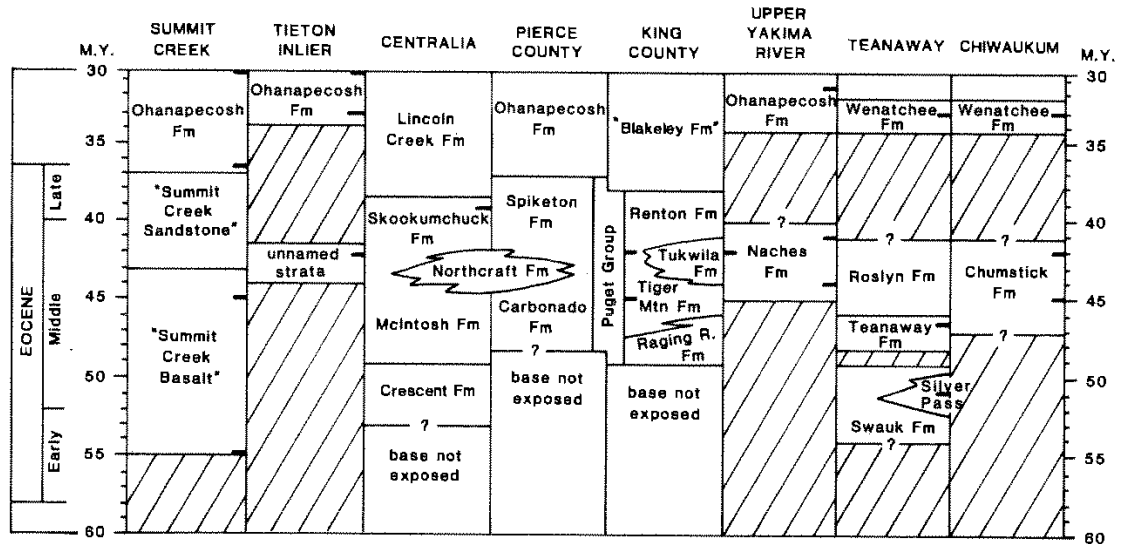


Fig. C.1 Stratigraphy of the regional basement of the Ohanapecosh Formation, copied from Vance et al. [1987].

GPS coordinates of the stratigraphic logs in the Ohanapecosh Formation

Section location		Latitude	Longitude	Altitude (mbsl)
Chinook Pass Member				
Gayuse Pass	start	46°51'19.2"N	121°31'32.7"W	1,282
	mid	46°51'21.7"N	121°31'37.2"W	1,336
	end	46°51'20.6"N	121°31'07.1"W	1,293
Chinook Pass	start	46°51'58.5"N	121°32'14.2"W	1,448
	mid	46°52'09.1"N	121°32'00.7"W	1,573
	end	46°52'35.7"N	121°31'45.2"W	1,653
Cougar Lake	A	46°49'14.3"N	121°28'31.3"W	1,759
	B1 start	46°48'50.4"N	121°27'37.9"W	1,739
	B1 end	46°48'44.6"N	121°27'41.7"W	1,827
	B2	46°48'44.4"N	121°27'23.7"W	1,843
White Pass Member				
White Pass	start	46°40'33.0"N	121°31'22.9"W	805
	mid 1	46°40'41.4"N	121°31'48.5"W	776
	mid 2	46°40'50.4"N	121°32'28.1"W	679
	mid 3	46°41'21.9"N	121°33'14.4"W	559
	end	46°41'07.8"N	121°34'45.8"W	491
Scoria cone at White Pass	cliff	46°41'21.9"N	121°33'14.4"W	559
Ohanapecosh campground	start	46°44'15.4"N	121°34'21.3"W	597
	mid	46°44'21.7"N	121°34'27.1"W	684
	end	46°44'28.9"N	121°34'33.1"W	816
Backbone Ridge	B start	46°44'52.4"N	121°34'14.0"W	822
	B end	46°44'42."N	121°34'14.5"W	838
	C start	46°44'31.8"N	121°34'36.3"W	906
	C end	46°44'11.4"N	121°34'45.7"W	918
	D start	46°43'47.6"N	121°35'02.2"W	942
	D end	46°43'30.1"N	121°35'12.6"W	972
Indian Bar	A	46°49'10.9"N	121°37'46.3"W	1,690
	B	46°49'15.4"N	121°37'53.2"W	1,745
Johnson Creek Member				
South Packwood	section	46°33'25.4"N	121°35'43.8"W	1,250
	leaves	46°25'46.0"N	121°33'05.9"W	1,266

APPENDIX D - DOGASHIMA FORMATION

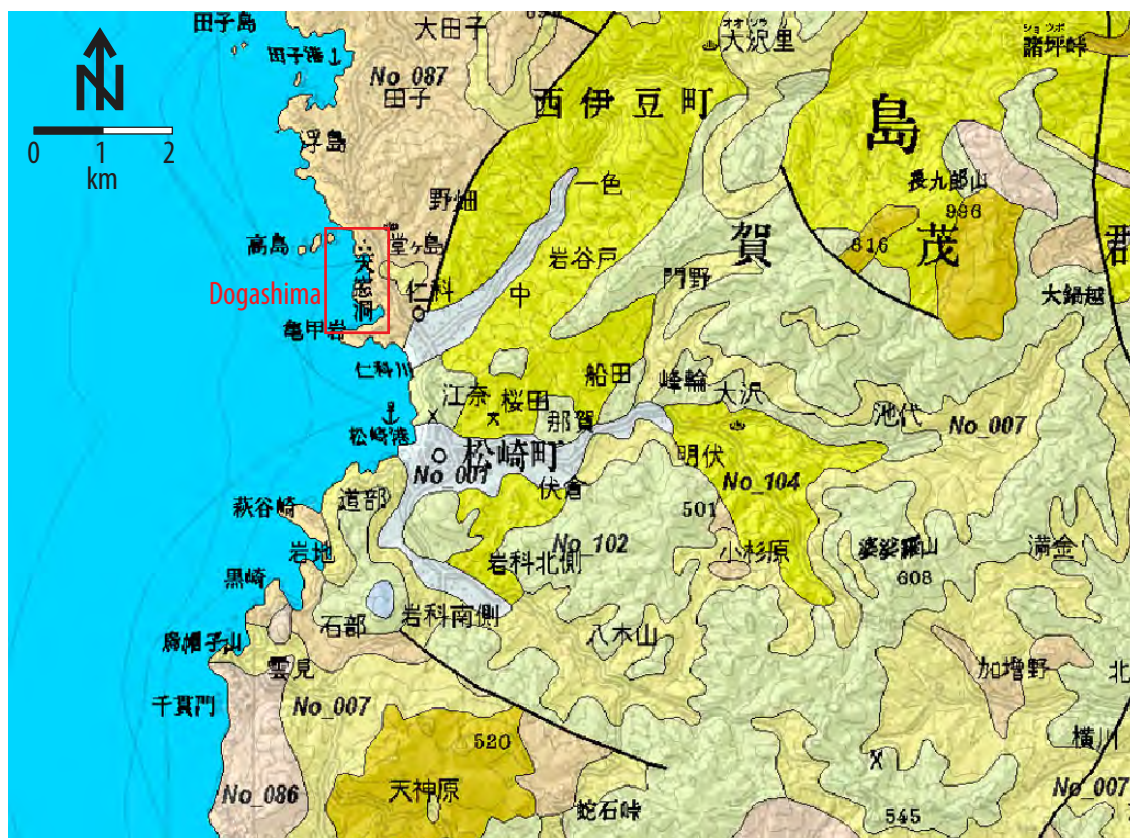


Fig. D.1 Geological map around the Dogashima Formation [Geological Survey of Japan, 2010]. Red box delimitates the map in Fig. 4.1b. 001: Late Pleistocene to Holocene; marine and non-marine sediments, 001; Middle to Late Miocene; non marine sediments, 007; Late Miocene to Pliocene; non-alkaline felsic volcanic rocks, 086; Middle to Late Miocene; non-alkaline felsic volcanic rocks, 087; Early Pleistocene; non-alkaline mafic volcanic rocks, 101; Late Miocene to Pliocene; non-alkaline mafic volcanic rocks, 102; Early to Middle Miocene; non-alkaline mafic volcanic rocks, 104.

Geochemistry of the Dogashima Formation

Composition of major elements in plagioclase phenocrysts and microlites in white pumice and grey andesite clasts in Dogashima 2, analysed on the Cameca 100X microprobe at the *Central Science Laboratory* of the University of Tasmania.

Sample	SiO ₂	TiO ₂	Al ₂ O ₃	FeO	MnO	MgO	CaO	Na ₂ O	K ₂ O	P ₂ O ₅	BaO	SrO	Cl	Total
Izu-15-GreyAnd-microl-1	54.45	0.01	29.26	0.36	0.00	0.04	11.67	4.82	0.11	0.01	0.00	0.07	0.00	100.80
Izu-15-GreyAnd-microl-2	54.94	0.00	29.02	0.37	0.02	0.08	11.08	4.97	0.12	0.03	0.01	0.06	0.00	100.68
Izu-15-GreyAndMicrol-3	56.48	0.00	28.03	0.27	0.00	0.03	9.99	5.67	0.17	0.00	0.04	0.06	0.00	100.74
Izu-15-GreyAndMicrol-4	54.60	0.00	29.23	0.36	0.01	0.11	11.44	5.11	0.14	0.00	0.02	0.05	0.01	101.09
Izu-15-GreyAndMicrol-5	56.48	0.01	28.00	0.29	0.00	0.05	10.24	5.47	0.16	0.01	0.06	0.03	0.01	100.81
Izu-15-GreyAndMicrol-6	55.63	0.01	28.59	0.36	0.00	0.09	10.77	5.04	0.09	0.03	0.00	0.05	0.00	100.67
Izu-15-GreyAndMicrol-7	56.49	0.01	28.37	0.31	0.00	0.06	10.45	5.48	0.11	0.05	0.00	0.02	0.00	101.35
Izu-15-GreyAndMicrol-8	55.35	0.01	28.53	0.36	0.02	0.04	10.86	5.21	0.18	0.00	0.00	0.07	0.00	100.65
Izu-15-GreyAndMicrol-9	55.61	0.00	28.85	0.35	0.01	0.06	10.74	5.42	0.16	0.08	0.00	0.08	0.01	101.37
Izu-15-GreyAndesite-10	52.95	0.04	30.45	0.43	0.01	0.09	12.74	4.38	0.12	0.00	0.00	0.02	0.00	101.23
Izu-15-GreyAndesite-11	50.65	0.02	31.53	0.66	0.01	0.12	14.20	3.56	0.03	0.01	0.00	0.01	0.00	100.79
Izu-15-GreyAndesite-12	54.89	0.01	28.86	0.40	0.02	0.09	10.95	5.19	0.13	0.02	0.06	0.05	0.01	100.68
Izu-15-GreyAndesite-13	52.66	0.01	30.93	0.39	0.01	0.03	13.11	4.02	0.08	0.04	0.00	0.01	0.00	101.29
Izu-15-GreyAndesite-15	55.16	0.00	29.02	0.41	0.01	0.06	11.06	5.06	0.20	0.01	0.01	0.05	0.00	101.04
Izu-31-GreyAndesite-5	53.23	0.01	30.27	0.38	0.00	0.18	12.36	4.20	0.06	0.00	0.06	0.07	0.00	100.82
Izu-31-GreyAndesite-7	55.74	0.00	28.75	0.41	0.02	0.14	10.94	5.11	0.18	0.03	0.03	0.02	0.02	101.38
Izu-31-GreyAndesite-8	54.87	0.00	29.07	0.32	0.00	0.06	11.34	5.11	0.12	0.01	0.01	0.06	0.00	100.99
Izu-31-GreyAndesite-10	53.05	0.00	30.56	0.42	0.03	0.05	12.76	3.97	0.10	0.01	0.00	0.14	0.00	101.08
Izu-31-GreyAndesite-11	54.21	0.03	29.44	0.38	0.00	0.07	11.74	4.81	0.08	0.00	0.00	0.01	0.00	100.77
Izu-31-GreyAndesite-13	51.62	0.03	30.70	0.92	0.03	0.09	13.64	3.83	0.09	0.00	0.00	0.00	0.01	100.95
Izu-31-GreyAndesite-14	53.66	0.03	30.11	0.56	0.02	0.03	12.73	3.98	0.12	0.02	0.00	0.05	0.00	101.31
Izu-31-GreyAndesite-15	51.56	0.03	30.35	0.72	0.00	0.06	13.32	3.52	0.15	0.00	0.00	0.06	0.00	99.79
Izu-31-WhitePumice-44	55.46	0.02	28.28	0.36	0.01	0.03	10.53	5.41	0.16	0.00	0.01	0.01	0.00	100.29
Izu-31-WhitePumice-45	56.85	0.00	28.26	0.34	0.00	0.02	9.92	5.73	0.19	0.00	0.03	0.03	0.01	101.39
Izu-31-WhitePumice-46	53.55	0.02	29.88	0.34	0.04	0.05	12.34	4.30	0.11	0.05	0.01	0.05	0.00	100.73
Izu-31-WhitePumice-51	55.73	0.00	28.31	0.35	0.00	0.04	10.40	4.84	0.09	0.00	0.00	0.06	0.01	99.82
Izu-31-WhitePumice-52	56.25	0.01	28.13	0.33	0.03	0.09	10.15	5.11	0.13	0.00	0.00	0.05	0.00	100.27
Izu-31-WhitePumice-55	56.49	0.00	27.96	0.35	0.00	0.04	10.15	5.37	0.12	0.00	0.00	0.08	0.00	100.56
Izu-31-WhitePumice-57	56.74	0.00	27.81	0.38	0.00	0.01	9.98	5.46	0.13	0.00	0.08	0.07	0.00	100.65
Izu-31-WhitePumice-58	52.63	0.02	30.60	0.46	0.00	0.05	13.19	4.03	0.09	0.01	0.00	0.07	0.00	101.13
Izu-31-WhitePumice-60	56.26	0.01	28.13	0.32	0.00	0.08	10.36	5.28	0.17	0.02	0.00	0.05	0.02	100.70
Izu-31-WhitePumice-62	55.97	0.01	28.79	0.37	0.03	0.06	10.82	5.15	0.07	0.01	0.00	0.06	0.02	101.36
Izu-31-WhitePumice-45b	51.29	0.01	31.58	0.41	0.00	0.02	14.06	3.28	0.08	0.00	0.01	0.05	0.01	100.79
Izu-31-FreeFeldspar-27	51.02	0.01	31.46	0.63	0.00	0.21	13.94	3.28	0.21	0.01	0.02	0.02	0.00	100.80
Izu-31-FreeFeldspar-28	55.51	0.02	28.58	0.36	0.00	0.03	10.50	5.29	0.24	0.00	0.07	0.08	0.01	100.68
Izu-31-FreeFeldspar-29	54.15	0.00	29.69	0.42	0.02	0.07	11.98	4.51	0.18	0.00	0.00	0.09	0.01	101.12
Izu-31-FreeFeldspar-33	55.54	0.00	28.70	0.39	0.01	0.07	10.83	5.57	0.14	0.02	0.00	0.05	0.00	101.32
Izu-31-FreeFeldspar-27b	50.12	0.04	32.07	0.42	0.03	0.05	14.63	3.35	0.05	0.02	0.04	0.03	0.01	100.85
Izu-31-RedGreyAnd-16	53.53	0.02	29.98	0.89	0.00	0.14	13.03	3.93	0.09	0.00	0.00	0.01	0.00	101.63
Izu-31-RedGreyAnd-18	48.88	0.01	32.80	0.60	0.00	0.09	15.58	2.80	0.01	0.00	0.00	0.09	0.02	100.87
Izu-31-RedGreyAnd-19	48.47	0.03	32.71	0.59	0.00	0.08	15.73	2.39	0.03	0.01	0.03	0.05	0.01	100.15
Izu-31-RedGreyAnd-23	52.58	0.01	30.36	0.47	0.00	0.07	12.79	3.85	0.17	0.02	0.00	0.03	0.00	100.36

APPENDIX E - MANUKAU SUB-GROUP, NEW ZEALAND

1.1 Geological setting of the Manukau Sub-Group

The Early Miocene Northland Volcanic Arc, New Zealand, is represented by the Waitakere Group (West) and the Coromandel Group (East), and the central Waitemata Group [Cole, 1986; Hayward, 1993; Hayward *et al.*, 2001; Allen *et al.*, 2007]. The Waitakere Group, emplaced between 25 and 15.5 Ma [K-Ar; Hayward *et al.*, 2001], consisted in two large (Manukau and Kaipara subgroups) and several minor submarine and terrestrial stratovolcanoes, and a large shield complex (Waipoua). Lavas and intrusions are mostly basaltic to andesitic; minor dacite and rhyolite are present [Wright and Black, 1981]. The NW elongation of the two belts and the typical calcalkaline compositions have been interpreted to indicate a convergent margin setting, related to the SW-directed subduction of the Pacific plate under the Australian plate [e.g. Cole, 1986; Hayward, 1993].

The Manukau Subgroup of the Waitakere Group consists of facies that accumulated on the submarine apron of an island stratovolcano, formerly 2-3 km high and 60x40 km across, now situated offshore ~60 km west of Auckland [Davey, 1974; Hatherton *et al.*, 1979; Allen *et al.*, 2007]. A consistent succession of proximal (present-day western coast) to distal (inland) volcanoclastic facies are exposed (Fig. F.1); lavas shallow intrusions mark the locations of satellite vents. The Waitakere Group conformably overlies the Waitemata Group turbidites which were deposited at bathyal (1,000-2,000 m) depths [Hayward, 1976a; 1979; Walker, 1992; Allen *et al.*, 2007].

The products of more than 7 million years of volcanism of the Manukau Subgroup is beautifully exposed in continuous coastal outcrops, and have been divided into five formations through multiple contributions [e.g. Hayward, 1976b; c; 1977; 1979; 1983; Hayward, 1993; Hayward *et al.*, 2001]. Allen *et al.* [2007] reviewed the stratigraphy and proposed a new approach, based on volcanic facies analysis. Four subaqueous (proximal, medial, distal and channel-fill) and one subaerial volcanic facies were described, all associated with the mostly submarine volcanic apron. A general summary is presented here.

The proximal facies, found in the Piha and Waiatarua Formations, are mostly bimodal in grain size. Coarse to very coarse facies ("coarse breccia-conglomerate, boulder conglomerate facies") are interbedded with much finer ones ("sandstone to granule sandstone"). The coarse grain size suggests a proximal setting (few kms) relative to the vent, whereas well rounded clasts indicate reworking in a subaerial or shallow marine setting. A facies of channel deposit is proposed for the coarse facies which show erosion, stratification and/or development in lenses. "Pillow lavas and their associated hyaloclastites" built tens-of-metres-thick units, cross-cut by "dykes". This association is representative of multiple

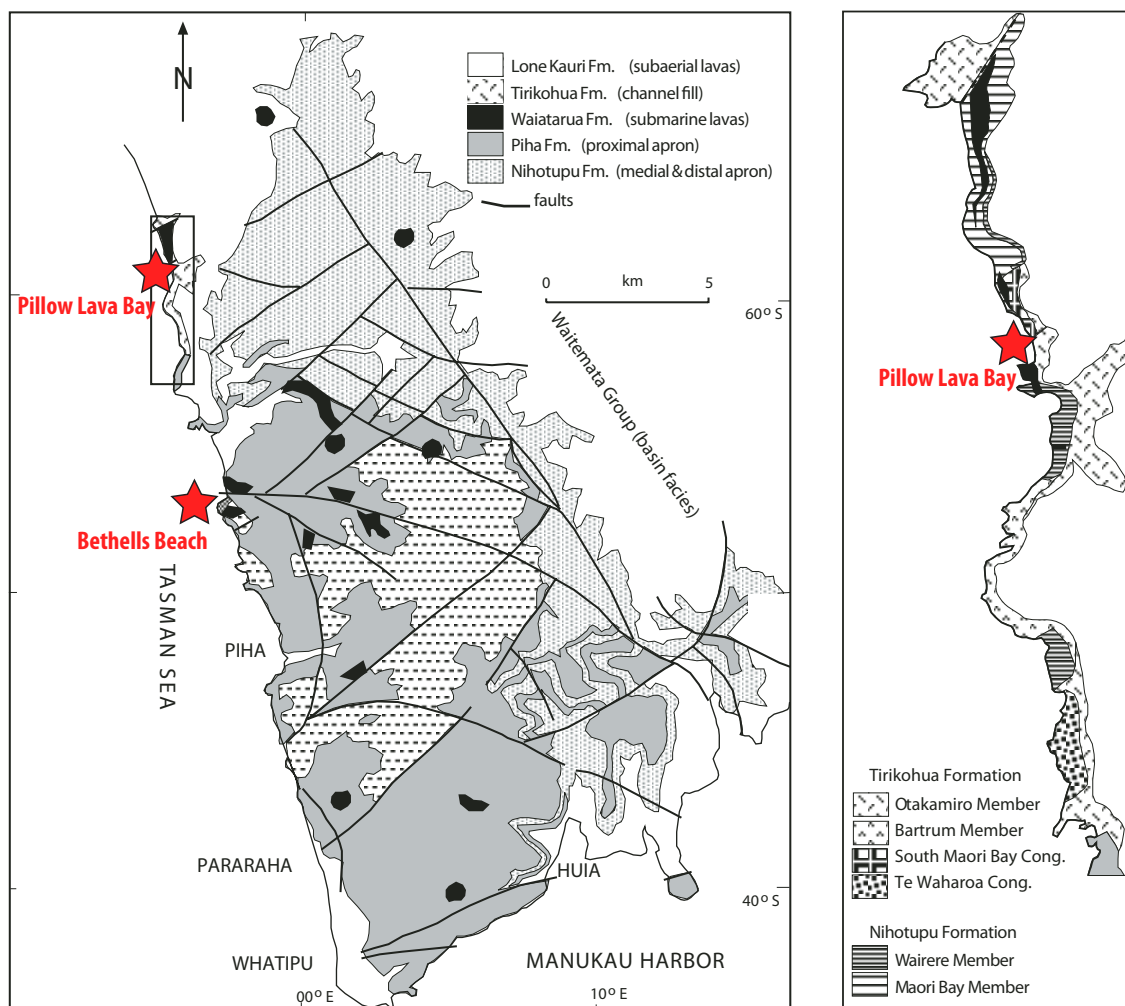


Fig. F.1 Geologic map of the Manukau Sub-Group, New Zealand. Simplified from Allen et al. [2007]. Outlined rectangle corresponds to right inset.

satellite vents around the major Manukau edifice. “Megabreccias”, consisting of large (100’s m) chaotically disrupted domains, are interpreted as debris-avalanche deposits, possibly derived from parts of the offshore cone. Some “pumice-rich” interbeds were interpreted to be water-settled fall deposits from submarine explosive eruptions, possibly subsequently remobilized. The medial and distal apron facies, represented by Nihotupu and Waiatarua Formations, are mostly composed of volcanoclastic facies. The “thinly-to medium-bedded” facies, in association with fine sandstone, were interpreted to be turbidites. Presence of coarse angular pumice provides from water-settling of subaerial fallout. Large volumes of “thinly to thickly bedded pumiceous pebbly sandstone” occur in the medial apron, and were interpreted to be deposited from topographically-confined high-density turbidity currents. “Poorly sorted conglomerates” denote occurrence of cohesive debris-flow deposits. Coherent (mega-)pillow lavas, sheet lavas and associated breccia facies are widely exposed and similar to those found in the proximal apron facies, and suggest the presence of multiple satellite vents. Walker [1992] included the pillow lavas at Muriwai in a worldwide study of pillow lava emplacement. The megapillows at Muriwai were also studied by Bear and Cas [2007].

Tirikohura and Waiatarua Formations show “intercalated, well rounded cobble/pebble conglomerate and stratified pebbly sandstone” and were deposited from high-density turbidity currents [Lowe, 1982] into a channel. The roundness of the clasts strongly suggests prior reworking in a subaerial or shoreline environment. The presence of coarse facies in an otherwise distal association could reflect an episode of significant erosion of the apron. Several mechanisms of transport are interpreted to have been involved in the deposition of “thin- and thick-bedded pebbly sandstone”. “Pumice facies” are also present and attributed to deposition from high-density turbidity currents. “Dyke and lobe” were interpreted to be very shallow intrusions.

The final stage of volcanism of the Manukau volcano produced in the Lone Kauri Formation, composed of “subaerial lavas and associated intrusions” above the proximal apron associations. This stage occurred after or during uplift and gentle folding of the older formations.

1.2 Application of image analysis and functional stereology

Outcrops of the Manukau Sub-Group at Bethells Beach and Pillow Lava Bay are two localities amenable (chapter 2) to grain size analysis (Fig. F.1), in which cement is easily distinguishable from fine clasts (<2 mm) forming the matrix. The successions are clast-supported, and contain large quantities of pumice clasts. The beds at Pillow Lava Bay are mostly composed of pumice clasts and matrix, and the content of dense clasts diminishes upwards in the stratigraphy (Fig. F.1). Pumice clasts dominate the basal beds at Bethells Beach. Upwards in the stratigraphy, the beds become richer in cement, as well as finer grained; pumice clasts are <2 mm and considered as matrix. Dense clasts are minor and fluctuate little in the stratigraphy.

The Manukau Sub-Group beds are dominated by pumice and dense clast distributions that have wider space separating modes (Fig. 5.2e). The Pillow Lava Bay sample is strongly depleted in 2–4 mm clasts (Fig. 5.2c), whereas clasts <2 mm and >4 mm are abundant. The beds of Bethells Beach are normally graded and components coarser than 4 mm disappear upwards (Fig. 5.1c), and the proportion of cement and matrix dramatically increases in volume (<10 to ~35 vol.%).

APPENDIX F - SAMPLE LIST

Samples catalogued at the University of Tasmania

UTas #	Sample	Geological unit	Locality	Unit/bed	Facies	Rock	XRF pill
173752	WA-03	Ohanapecosh Formation, WA, USA	White Pass	30	5	yes	
173753	WA-06	Ohanapecosh Formation, WA, USA	White Pass	47	9	yes	
173754	WA-07	Ohanapecosh Formation, WA, USA	White Pass	62	6	yes	
173755	WA-08	Ohanapecosh Formation, WA, USA	White Pass	122	16	yes	
173756	WA-09	Ohanapecosh Formation, WA, USA	White Pass	137	10	yes	
173757	WA-10	Fifes Peak Formation, WA, USA	Low White Pass	143	red fiam bx, Stev. Ridge Mm.	yes	
173758	WA-11	Fifes Peak Formation, WA, USA	Low White Pass	143	red fiam bx, Stev. Ridge Mm.	yes	
173759	WA-15	Ohanapecosh Formation, WA, USA	Cayuse Pass	top 43	2	yes	
173760	WA-16	Ohanapecosh Formation, WA, USA	Cayuse Pass	mid 43	2	yes	
173761	WA-17	Ohanapecosh Formation, WA, USA	Cayuse Pass	base 43	2	yes	
173762	WA-21	Ohanapecosh Formation, WA, USA	Cayuse Pass	top 40	1	yes	
173763	WA-22	Ohanapecosh Formation, WA, USA	Cayuse Pass	mid 40	1	yes	
173764	WA-23	Ohanapecosh Formation, WA, USA	Cayuse Pass	base 40	1	yes	
173765	WA-30	Ohanapecosh Formation, WA, USA	Chinook Pass	1	-	yes	
173766	WA-37	Ohanapecosh Formation, WA, USA	Chinook Pass	57 mid	3	yes	
173767	WA-39	Ohanapecosh Formation, WA, USA	Chinook Pass	59 base	4	yes	
173768	WA-41	Ohanapecosh Formation, WA, USA	Chinook Pass	59 mid	4	yes	
173769	WA-44	Ohanapecosh Formation, WA, USA	Chinook Pass	59 top	4	yes	
173770	WA-46	Ohanapecosh Formation, WA, USA	Chinook Pass	60b mid	12	yes	
173771	WA-60	Ohanapecosh Formation, WA, USA	Backbone B	2	5	yes	
173772	WA-66	Ohanapecosh Formation, WA, USA	Chinook Pass	61 base	4	yes	
173773	WA-67	Ohanapecosh Formation, WA, USA	Chinook Pass	61 mid 1	4	yes	
173774	WA-70	Ohanapecosh Formation, WA, USA	Chinook Pass	61 top	4	yes	
173775	WA-89	Ohanapecosh Formation, WA, USA	Cougar Lake A	-	-	yes	
173776	WA-97	Ohanapecosh Formation, WA, USA	Indian Bar	7	-	yes	
173777	WA-98	Ohanapecosh Formation, WA, USA	White Pass	5	5	yes	
173778	IZU-03	Dogashima Fm. Izu Pen., Japan	Dogashima, A	D2-2	White pumice		yes
173779	IZU-04	Dogashima Fm. Izu Pen., Japan	Dogashima, A	D2-2	Grey andesite bx		yes
173780	IZU-05	Dogashima Fm. Izu Pen., Japan	Dogashima, A	D2-2	Grey andesite bx	yes	yes
173781	IZU-07	Dogashima Fm. Izu Pen., Japan	Dogashima, A	D2-2	Hydroth alt volc	yes	
173782	IZU-08	Matsuzaki Fm. Izu Pen., Japan	Matsuzaki, A	Matsuzaki	Dark andesite	yes	yes
173783	IZU-12	Dogashima Fm. Izu Pen., Japan	Dogashima, B	D1-2	Pum breccia	yes	
173784	IZU-13	Dogashima Fm. Izu Pen., Japan	Dogashima, B	D1-9	shard rich siltst	yes	
173785	IZU-15	Dogashima Fm. Izu Pen., Japan	Dogashima, B	D2-2	Grey andesite bx	yes	
173786	IZU-17	Dogashima Fm. Izu Pen., Japan	Dogashima, B	D1-2	Pum breccia	yes	
173787	IZU-24	Dogashima Fm. Izu Pen., Japan	Dogashima, D	D1-3	Polymictic volc breccia		yes
173788	IZU-25	Dogashima Fm. Izu Pen., Japan	Dogashima, D	D1-3	Polymictic volc breccia	yes	yes
173789	IZU-26	Dogashima Fm. Izu Pen., Japan	Dogashima, D	D1-6	Cross bedded bx/sst		yes
173790	IZU-27	Dogashima Fm. Izu Pen., Japan	Dogashima, D	D1-7	Polymictic volc breccia	yes	
173791	IZU-29	Dogashima Fm. Izu Pen., Japan	Dogashima, G	D2-b	White pum breccia	yes	
173792	IZU-30	Dogashima Fm. Izu Pen., Japan	Dogashima, G	D2-d	White pum breccia	yes	yes
173793	IZU-31	Dogashima Fm. Izu Pen., Japan	Dogashima, G	D2-b	White pum breccia	yes	
173794	IZU-32	Dogashima Fm. Izu Pen., Japan	Dogashima, G	D2-e	White pum breccia	yes	
173795	IZU-33	Dogashima Fm. Izu Pen., Japan	Dogashima, G	D2-e	White pum breccia	yes	
173796	IZU-34	Dogashima Fm. Izu Pen., Japan	Dogashima, G	D2-e	White pum breccia	yes	
173797	IZU-35	Dogashima Fm. Izu Pen., Japan	Dogashima, G	D2-4a	Stratif pum breccia	yes	
173798	IZU-37	Dogashima Fm. Izu Pen., Japan	Dogashima, G	D2-3e	White pum breccia	yes	
173799	IZU-39	Dogashima Fm. Izu Pen., Japan	Dogashima, G	D2-6	Cross-bedded pum brec-congl	yes	
173800	IZU-42	Dogashima Fm. Izu Pen., Japan	Dogashima, I	D3	Weakly stratif and bx	yes	yes

UTas #	Sample	Geological unit	Locality	Unit/ bed	Facies	Rock	XRF pill
173801	IZU-45	Dogashima Fm. Izu Pen., Japan	Dogashima, I	D2-7	Planar bedded pum bx		yes
173802	IZU-51	Dogashima Fm. Izu Pen., Japan	Dogashima, F	D2-2	Grey andesite bx		yes
173803	IZU-52	Dogashima Fm. Izu Pen., Japan	Dogashima, A	D2-2	Grey andesite bx		yes
173804	IZU-55	Dogashima Fm. Izu Pen., Japan	Dogashima, H	D2-6	Cross-bedded pum brec-congl	yes	yes
173805	IZU-56	Dogashima Fm. Izu Pen., Japan	Dogashima, G	D2-2	Grey andesite	yes	
173806	NZ-13	Manukau Sub-Grp, New Zealand	Bethells beach	13	Pumice lapillistone	yes	
173807	NZ-14	Manukau Sub-Grp, New Zealand	Bethells beach	14	Pumice lapillistone	yes	
173808	NZ-15	Manukau Sub-Grp, New Zealand	Bethells beach	15	Pumice lapillistone	yes	
173809	NZ-16	Manukau Sub-Group, New Zealand	Bethells beach	16	Pumice lapillistone	yes	
173810	NZ-21	Manukau Sub-Group, New Zealand	Bethells beach	21	Pumice lapillistone	yes	

